

Supporting Information

β -peptide bundles with fluororous cores

Matthew A. Molski,[†] Jessica L. Goodman,[†] Cody J. Craig, He Meng,[‡] Krishna Kumar,^{‡,§} and Alanna Schepartz^{†#,*}

Departments of [†]Chemistry and [#]Molecular, Cellular and Developmental Biology, Yale University, New Haven, Connecticut 06520-8107, and [‡]Department of Chemistry, Tufts University, Medford, MA 02155-5813, and [§]Cancer Center, Tufts Medical Center, Boston, MA 02111-1533

General Methods. Wang resin and all Fmoc-protected α -amino acids and were purchased from Novabiochem (San Diego, CA), except for Fmoc-5,5,5',5',5'-hexafluoroleucine, which was synthesized as described.¹ (7-Azabenzotriazol-1-yloxy)tripyrrolidino-phosphonium hexafluorophosphate (PyAOP) was purchased from Oakwood Products, Inc. (West Columbia, SC). 1-Hydroxy-7-azabenzotriazole (HOAt) was purchased from Chempep, Inc. (Miami, FL). Dimethylformamide (DMF), *N*-methyl-2-pyrrolidone (NMP), *N*-methyl morpholine (NMM), trifluoroacetic acid (TFA) and piperdine (Pip) were purchased from American Bioanalytical (Natick, MA). All other reagents were purchased from Sigma-Aldrich (St. Louis, MO). Mass spectra were acquired with an Applied Biosystems Voyager-DE Pro MALDI-TOF mass spectrometer (Foster City, CA). Reverse-phase HPLC was performed using a Varian Prostar HPLC and Vydac analytical (C8, 300 Å, 5 μ m, 4.6 mm X 150 mm) or semi-preparative (C8, 300 Å, 10 μ m, 10 mm X 250 mm) columns, using water/acetonitrile gradients containing 0.1% TFA. Circular dichroism (CD) spectra were acquired with a Jasco J-810 Spectropolarimeter (Jasco,

Tokyo, Japan) equipped with a Peltier temperature control. Analytical ultracentrifugation (AU) was performed using a Beckman XL-I instrument. All experiments were performed in phosphate

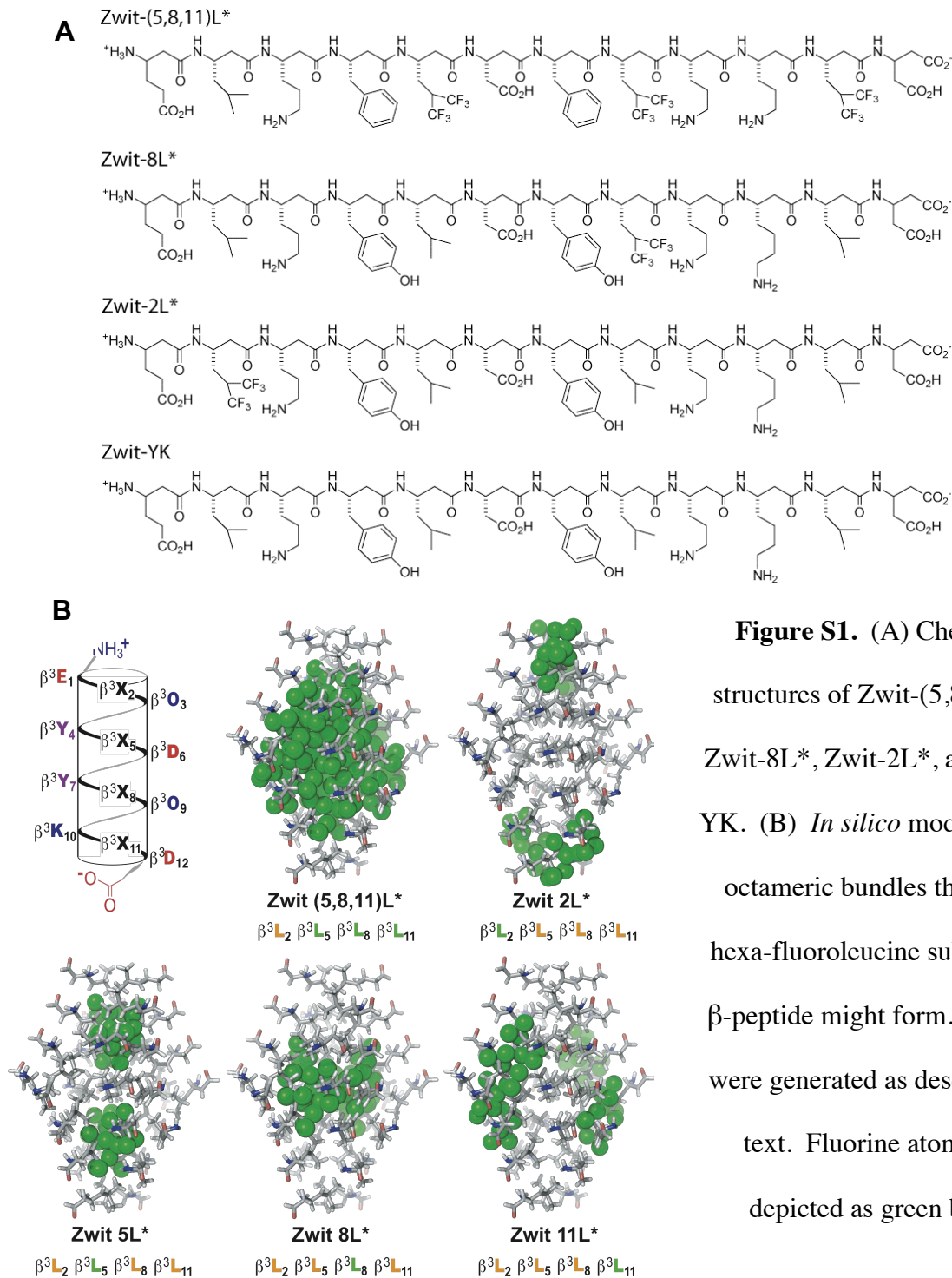


Figure S1. (A) Chemical structures of Zwit-(5,8,11)L*, Zwit-8L*, Zwit-2L*, and Zwit-YK. (B) *In silico* models of the octameric bundles that each hexa-fluoroleucine substituted β -peptide might form. Models were generated as described in text. Fluorine atoms are depicted as green balls.

buffer (10 mM NaH₂PO₄, 200 mM NaCl, pH adjusted to 7.1 with NaOH), except as noted.

β-peptide synthesis and purification. Fmoc-protected β³-amino acids were prepared according to methods described by Seebach.² β³-peptides were synthesized in a CEM MARS microwave reactor on a 25 μmole scale using standard Fmoc chemistry and Wang resin loaded with β³-homoaspartic acid as previously described.³ Microwave irradiation was conducted at a maximum power of 400 W and was monitored using a fiber optic temperature sensor. Reactions were agitated by magnetic stirring during irradiation. One cycle of peptide elongation consisted of the following steps: First, the loaded resin was washed manually with dimethylformamide (DMF) and the terminal Fmoc group was removed with 20% Pip/DMF (50% power at 400 W maximum, 70 °C, ramp 2 min, hold 4 min). The deprotected resin was then washed with DMF and treated with a cocktail containing 3 eq PYAOP, 3 eq HOAt, and 8 eq diisopropylethylamine (DIEA) (50% power at 400 W maximum, 60 °C, ramp 2 min, hold 6 min). The coupled resin was then washed extensively with DMF. These steps were repeated until the β-peptide sequence was complete. Following removal of the final Fmoc protecting group, the resin was washed alternately with DMF and methanol for a total of 16 washes, followed by an additional 8 consecutive methanol washes, and dried at least 30 min under N₂. The dry resin was then treated with three 4 mL portions of a cleavage cocktail containing 2% v/v water, 2% v/v phenol, and 2% v/v triisopropylsilane in TFA for 1 h, 1 h, and 30 min. Once the cleaved β-peptide was collected it was concentrated by rotary evaporation and reconstituted in H₂O/CH₃CN (1:1).

The success of each synthesis was assessed by both HPLC and MALDI-TOF analysis of the crude reaction mixture. β-peptides were then purified to homogeneity by reverse-phase HPLC. The identities and purities of the purified β-peptides were assessed by analytical HPLC and mass

spectrometry. MALDI mass spectra were obtained using peptide samples in α -cyano-4-hydroxycinnamic acid (CHCA) matrix. The masses found were: Zwit-(5,8,11)L* (m/z calculated, observed): [M+H]⁺ 1958, 1962; Zwit-8L* (m/z calculated, observed): [M+H]⁺ 1788, 1792; Zwit-2L* (m/z calculated, observed): [M+H]⁺ 1788, 1789. Following purification, β -peptides were lyophilized and reconstituted in buffer (10 mM Na₂HPO₄, 200 mM NaCl, pH adjusted to 7.1 with NaOH) for characterization.

Circular Dichroism (CD). Wavelength dependent CD spectra were acquired for various concentrations of Zwit-(5,8,11)L* (Figure S2A), Zwit-8L* (Figure 2A) and Zwit-2L* (Figure S2B) at 25 °C in continuous scan mode with 0.5 nm data pitch, 50 nm/min scanning speed, 4 sec response, 0.5 nm band width and 3 accumulations. The spectra for Zwit-(5,8,11)L* at all concentrations between 25 and 150 μ M lacked the expected minimum at 214 nm that is expected for 14-helices (see Figure S2A). The concentration dependence of the molar residue ellipticity (MRE) minima (\sim 214 nm for Zwit-8L* and 211 nm for Zwit-2L*) was determined by least-squares fitting of the total peptide monomer concentration as a function of experimental MRE in KaleidaGraph (Synergy Software; Reading, PA) with the following equation:⁴

$$[\text{Peptide}]_{\text{Total}} = \left\{ \frac{(\text{MRE}_{\text{Exp}} - \text{MRE}_{\text{Mon}})(1/K_a)}{n(\text{MRE}_{\text{Nmer}} - \text{MRE}_{\text{Mon}}) \left[1 - \left(\frac{\text{MRE}_{\text{Exp}} - \text{MRE}_{\text{Mon}}}{\text{MRE}_{\text{Nmer}} - \text{MRE}_{\text{Mon}}} \right)^n \right]} \right\}^{1/(n-1)}$$

The values obtained for the Zwit-8L* fitted parameters were $\text{MRE}_{\text{Mon}} = 2500 \text{ deg}\cdot\text{cm}^2\cdot\text{dmol}^{-1}$ (constant, not fit in equation), $\text{MRE}_{\text{8mer}} = 21358 \pm 444 \text{ deg}\cdot\text{cm}^2\cdot\text{dmol}^{-1}$, and $\ln K_a = 83.91 \pm 0.56$. The curve in Figure 2B was fit using these parameters. Zwit-2L* fitted parameters were $\text{MRE}_{\text{Mon}} = 1000 \text{ deg}\cdot\text{cm}^2\cdot\text{dmol}^{-1}$ (constant, not fit in equation), $\text{MRE}_{\text{4mer}} = 28943 \pm 416 \text{ deg}\cdot\text{cm}^2\cdot\text{dmol}^{-1}$,

and $\ln K_a = 34.27 \pm 0.20$. The curve in Figure S2C was fit using these parameters. Wavelength-dependent CD spectra for both Zwit-8L* and Zwit-2L* show a concentration dependent increase in helical structure, analogous to that observed for previously characterized octameric β -peptide bundles.⁵⁻⁸

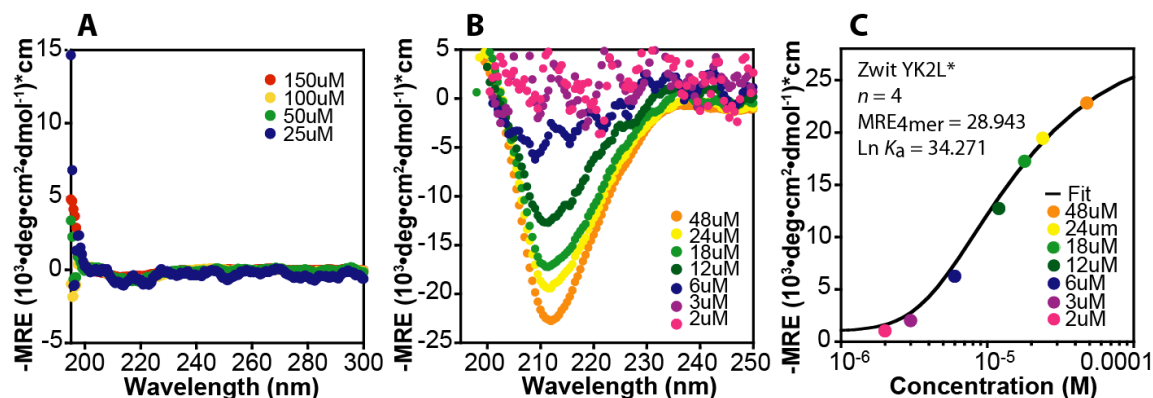


Figure S2. Self-association of β -peptides Zwit-2L* and Zwit-(5,8,11)L* monitored by wavelength-scan circular dichroism (CD) spectroscopy. (A) Zwit-(5,8,11)L* displays no evidence of 14-helicity at concentrations between 25 and 150 μM . (B) Wavelength-dependent CD spectra of Zwit-2L* at the indicated [Zwit-2L*] (μM). (C) Plot of MRE_{\min} as a function of [Zwit-2L*]_{monomer} fit to a monomer-tetramer equilibrium.

Temperature-dependent CD spectra of Zwit-8L* at various concentrations (6.25 μM , 12.5 μM , 25 μM , 50 μM , and 75 μM) were obtained at 214 nm between 10 and 95°C, using the variable temperature module provided with the instrument (Figure S3A). Data were collected with a 1°C data pitch, 10 sec delay time, 30 °C/h temperature slope, 4 sec response time, and 1 nm bandwidth. The first derivatives of the temperature-dependent CD spectra for the various concentrations of Zwit-8L* were calculated and the T_m values reported correspond to the maximum of the $\delta\text{MRE}_{214}/\delta T$ plots. Refer to Figure 2D for a plot of the $\delta\text{MRE}_{214}/\delta T$ as a

function of temperature for Zwit-8L* and Figure S3C for a plot of $\delta\text{MRE}_{214}/\delta T$ as a function of temperature for Zwit-2L*. T_m values for Zwit-8L* and Zwit-2L* are compared to those of Zwit-YK in Table S1.

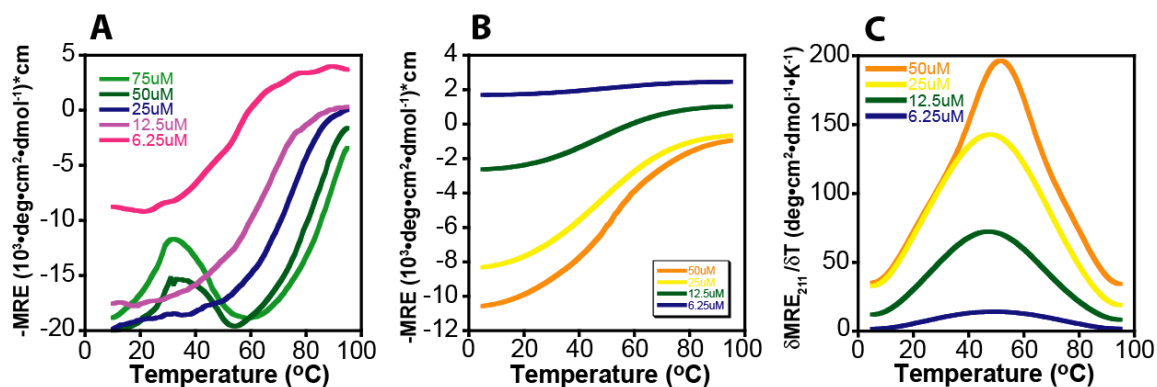
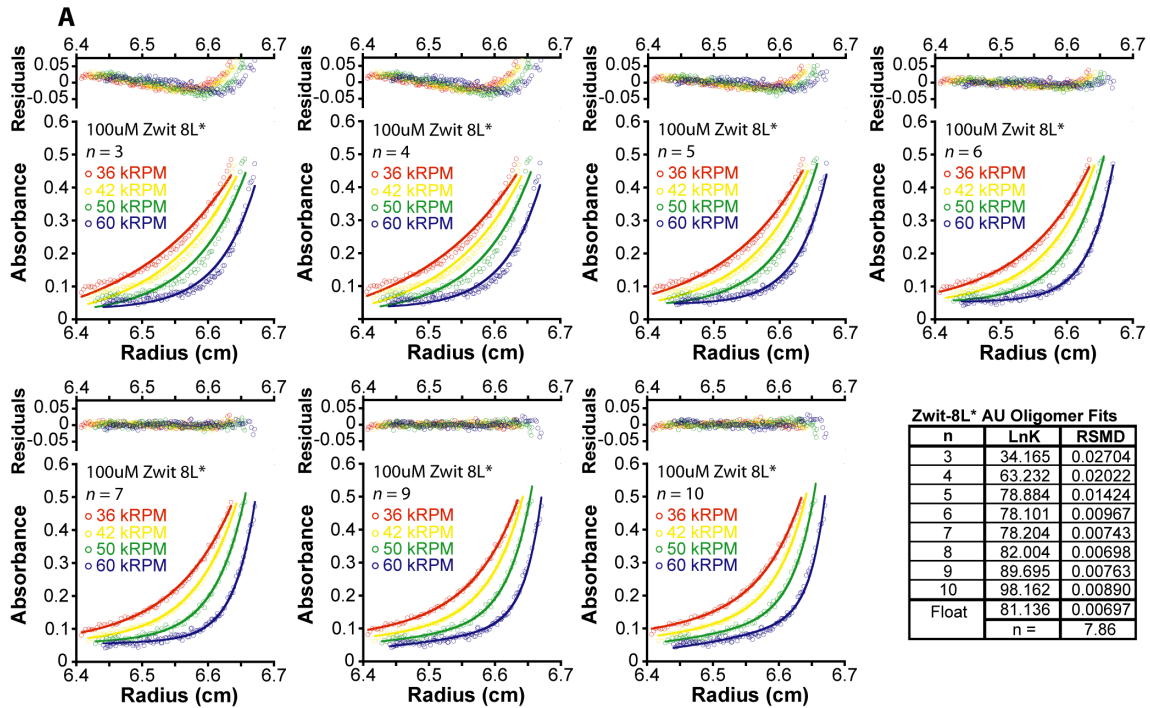


Figure S3. Zwit-8L* and Zwit-2L* self-association monitored by temperature melt circular dichroism spectroscopy (CD). (A) Temperature-dependent CD analysis of Zwit-8L* shown as a plot of MRE_{214} as a function of temperature at the indicated $[\text{Zwit-8L}^*]$ (μM). (B) Temperature-dependent CD analysis of Zwit-2L* shown as a plot of MRE_{211} as a function of temperature at the indicated $[\text{Zwit-2L}^*]$ (μM). (C) Plot of $\delta\text{MRE}_{209}/\delta T$ for the concentrations of Zwit-2L* shown in Figure S3B.

Conc. (μM)	T_m ($^{\circ}\text{C}$)		
	Zwit YK	Zwit 8L*	Zwit 2L*
6.25	60	54	49
12.5	68	65	47
25	77	74	48
50	85	82	52
75	-	>95	-

Table S1. Comparison of melting temperatures (T_m) for related β -peptides, Zwit-YK, Zwit-8L*, and Zwit-2L*. The Zwit-YK and Zwit-8L* octamers have similar T_m values at each concentration, whereas the Zwit-2L* tetramer melts at significantly lower temperatures.

Sedimentation Equilibrium Analytical Ultracentrifugation. HPLC-purified, lyophilized samples of Zwit-8L* (75 μ M, 100 μ M and 150 μ M) and Zwit-2L* (5 μ M, 25 μ M and 50 μ M; lower than Zwit-8L* due to low solubility) were resuspended and centrifuged at 25 $^{\circ}$ C to equilibrium at four different speeds (36,000, 42,000, 50,000 and 60,000 rpm). Centrifugation was performed in an AN 60-Ti 4-hole rotor equipped with six-channel, carbon-epoxy composite centerpieces (Beckman). Absorbance was monitored at 280 nm. Data were collected with a step size of 0.001 cm with scans occurring at 3 h intervals. Equilibration of the samples was determined when no significant change in radial concentration was observed in the successive scans using the program Match within the Heteroanalysis software suite (available from the National Analytical Ultracentrifugation Facility website, <http://www.biotech.uconn.edu/auf/>). The partial specific volume of each β -peptide was calculated from functional group composition according to Durchschlag and Zipper⁹.



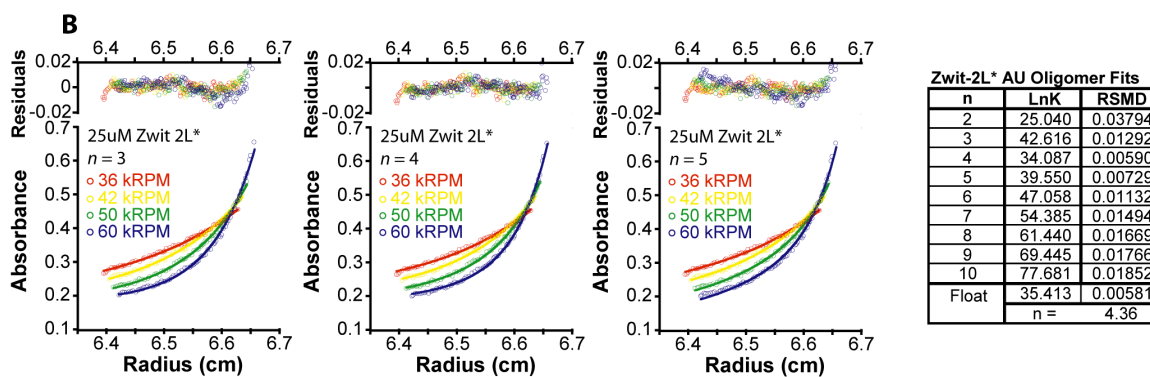


Figure S4. Sedimentation equilibrium analytical ultracentrifugation (AU) analysis of Zwit-8L* and Zwit-2L*. (A) The data for Zwit-8L* best fits a monomer-octamer equilibrium. (B) The data for Zwit-2L* best fits a monomer-tetramer equilibrium.

The data was fit to a monomer- n -mer equilibrium model using the Heteroanalysis software. Fixed parameters: Zwit-8L* monomer MW = 1788 Da, \bar{v} = 0.7610 cm³/g, d = 1.00674 g/mL, ϵ_{280} = 2980 M⁻¹•cm⁻¹, and n = 8; Zwit-2L* monomer MW = 1788 Da, \bar{v} = 0.7610 cm³/g, d = 1.00674 g/mL, ϵ_{280} = 2980 M⁻¹•cm⁻¹, and n = 4; Fitted parameters: Zwit-8L* $\ln K_a$ = 82.004 \pm 0.25, RMSD = 0.00698 and baseline deviation <0.02; Zwit-2L* $\ln K_a$ = 34.087 \pm 0.14, RMSD = 0.00590 and baseline deviation <0.02. The data shown (Figures 2C and S5) were fit with these parameters and the resulting residuals. Both peptides were also fit to n values of 2 though 10 with $\ln K_a$ and RMSD values shown in Figure S4A & B.

1-anilino-8-naphthalenesulfonate (ANS) Binding. A stock solution of 200 μ M Zwit-8L* plus 10 μ M ANS was prepared in phosphate buffer (10 mM Na₂HPO₄, 200 mM NaCl, pH 7.1). A 10 μ M solution of ANS was prepared in the phosphate buffer (from an initial stock of 500 μ M ANS) to be used for subsequent dilutions. Using serial dilutions, the binding of ANS to Zwit-8L* was measured at peptide concentrations ranging from 200 μ M down to 244 pM, in order to replicate the concentrations used for Zwit-YK. Fluorescence intensity (counts/s) measurements

were made using a Photon Technology International (Lawrenceville, NJ) Quantamaster C-60 spectrofluorimeter at 25 °C in a 1 cm path length Hellma (Mullheim, Germany) cuvette. The sample was excited with 350 nm light (4 nm slit width) and fluorescence emission was measured at 1 nm intervals between 400 and 600 nm (Figure S5A). The fluorescence ratio was calculated as the total fluorescence at each peptide concentration relative to fluorescence in the absence of peptide (10 μ M ANS). The fluorescence ratio of Zwit-8L* was larger than that of Zwit-YK at each concentration until both reached an asymptote at the baseline level.

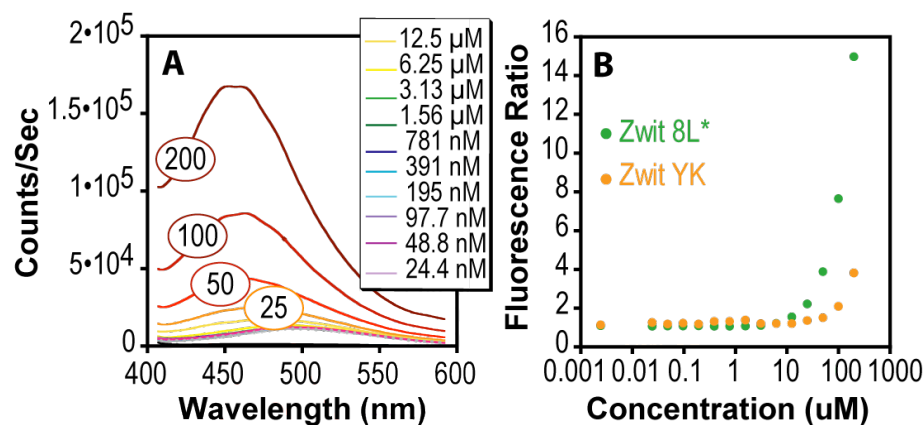


Figure S5.

Fluorescence of 1-anilino-8-naphthalenesulfonate (ANS) upon binding to Zwit-8L*.

(A) Change in fluorescence of 10 μ M ANS in the presence of the indicated concentration of Zwit-8L*.

Binding reactions were prepared in a buffer composed of 10 mM Na₂HPO₄, 200 mM NaCl (pH 7.1). (B). Ratio of ANS fluorescence in the presence of given concentrations of Zwit-8L* and Zwit-YK.

Crystallization and Structure Determination. Zwit-8L* (1.0 mM) was crystallized by hanging drop vapor diffusion over a mother liquor of 0.1 M sodium dihydrogen phosphate, 0.1 M potassium dihydrogen phosphate, 0.1 M MES pH 6.5 and 2.0 M sodium chloride. Crystals were cryoprotected using a step-wise transfer from mother liquor containing 0% glycerol to mother liquor supplemented with 7.5% glycerol. X-ray diffraction data to 1.7 Å resolution was

collected at 100K at the Yale Center for Structural Biology. Data was processed to 2.75 Å resolution using the HKL2000 software suite.¹⁰ Phases for Zwit-8L* were obtained by molecular replacement starting with a tetramer of the previously solved Zwit-1F octamer⁷ to 2.75 Å using CNS. Density modification and NCS averaging were performed using CNS.¹¹ The program XFIT was used to build and refine eight 3_{14} -helices into the electron density maps.¹² Refinement was performed using CNS with an R_{free} set to 10% of the data.¹¹ We found it challenging to successfully refine the structure, which caused us to re-examine our collected diffraction data. During this process, we found that our data was translationally twinned, which could not be deconvoluted using traditional detwinning methods (Yeates, CCP4 or CNS). For this reason, we examined the maps from our initial phasing efforts without proceeding with structure refinement. These maps clearly show the substantial electron density exclusively in the region of the hexafluoroleucine residues (position 8), validating that our maps are not biased by our model structure used in molecular replacement (Figure 3). PyMOL was used for figure preparation.¹³

References cited

- (1) Xing, X.; Fichera, A.; Kumar, K. *Org Lett* **2001**, *3*, 1285-6.
- (2) Seebach, D.; Overhand, M.; Kuhnle, F. N. M.; Martinoni, B.; Oberer, L.; Hommel, U.; Widmer, H. *Helv. Chim. Acta* **1996**, *79*, 913-941.
- (3) Hart, S. A.; Bahadoor, A. B.; Matthews, E. E.; Qiu, X. J.; Schepartz, A. *J Am Chem Soc* **2003**, *125*, 4022-3.
- (4) Degrado, W. F.; Lear, J. D. *J. Am. Chem. Soc.* **1985**, *107*, 7684-7689.
- (5) Goodman, J. L.; Petersson, E. J.; Daniels, D. S.; Qiu, J. X.; Schepartz, A. *J Am Chem Soc* **2007**, *129*, 14746-51.
- (6) Petersson, E. J.; Craig, C. J.; Daniels, D. S.; Qiu, J. X.; Schepartz, A. *J Am Chem Soc* **2007**, *129*, 5344-5.
- (7) Daniels, D. S.; Petersson, E. J.; Qiu, J. X.; Schepartz, A. *J Am Chem Soc* **2007**, *129*, 1532-3.
- (8) Qiu, J. X.; Petersson, E. J.; Matthews, E. E.; Schepartz, A. *J. Am. Chem. Soc.* **2006**, *128*, 11338-11339.
- (9) Durchschlag, H.; Zipper, P. In *Ultracentrifugation*; Lechner, M. D., Ed.; Dr Dietrich Steinkopff Verlag: Berlin 33, 1994; Vol. 94, p 20-39.

- (10) Otwinowski, Z.; Minor, W. In *Macromolecular Crystallography, Pt A*; Academic Press Inc: San Diego, 1997; Vol. 276, p 307-326.
- (11) Brunger, A. T.; Adams, P. D.; Clore, G. M.; DeLano, W. L.; Gros, P.; Grosse-Kunstleve, R. W.; Jiang, J. S.; Kuszewski, J.; Nilges, M.; Pannu, N. S.; Read, R. J.; Rice, L. M.; Simonson, T.; Warren, G. L. *Acta Crystallogr. Sect. D-Biol. Crystallogr.* **1998**, *54*, 905-921.
- (12) McRee, D. E. *J. Struct. Biol.* **1999**, *125*, 156-165.
- (13) DeLano, W. L. *The PyMOL Molecular Graphics System* **2002**, DeLano Scientific, San Carlos, CA, USA.